

The hematite ($\alpha\text{-Fe}_2\text{O}_3$) (0001) surface: evidence for domains of distinct chemistry

X.-G. Wang, W. Weiss, Sh. K. Shaikhutdinov, M. Ritter, M. Petersen, F. Wagner, R. Schlögl, and M. Scheffler
Fritz-Haber-Institut der Max-Planck-Gesellschaft, Faradayweg 4-6, D-14195 Berlin-Dahlem, Germany
 (November 26, 2024)

Using spin-density functional theory we investigated various possible structures of the hematite (0001) surface. Depending on the ambient oxygen partial pressure, two geometries are found to be particularly stable under thermal equilibrium: one being terminated by iron and the other by oxygen. Both exhibit huge surface relaxations (-57% for the Fe- and -79% for the O-termination) with important consequences for the surface electronic and magnetic properties. With scanning tunneling microscopy we observe two different surface terminations coexisting on single crystalline $\alpha\text{-Fe}_2\text{O}_3$ (0001) films, which were prepared in high oxygen pressures.

PACS numbers:68.35.Bs,61.16.Ch,68.35.Md,71.15.Ap

Although metal-oxide surfaces play a crucial role for several profitable processes, good quality experimental and theoretical studies of their atomic structure and electronic properties are scarce. For example, $\alpha\text{-Fe}_2\text{O}_3$ appears to be the active catalytic material for producing styrene,¹ which was substantiated by recent reactivity studies performed over single crystalline hematite model catalyst films.² Other candidate applications are photoelectrodes³ and non-linear optics materials⁴. Nevertheless, the surface properties of $\alpha\text{-Fe}_2\text{O}_3$ are basically unknown, and also for other metal oxides an understanding is developed only badly. The reason is the difficult preparation of clean surfaces with defined structures and stoichiometries, which, as in the case of hematite, can require high oxygen pressures not suitable in standard ultrahigh vacuum systems. Furthermore, electron spectroscopy techniques and scanning tunneling microscopy (STM) are hampered by the insulating nature of the material. We also note that surface-science techniques often do not probe a thermal equilibrium geometry but a frozen-in metastable state. Theoretical studies, on the other hand, have to deal with $3d$ electrons, oxygen with very localized wave functions, a rather open structure, unusual hybridization of wave functions, huge atomic relaxations, big super cells, and magnetism. This renders an *ab initio* study of $\alpha\text{-Fe}_2\text{O}_3$ surfaces a most challenging investigation. Some theoretical studies of the geometry of $\alpha\text{-Fe}_2\text{O}_3$ (0001) had been performed using empirical (classical) potentials^{5,6}, and Armelao *et al.*⁷ studied the electronic structure employing a cluster approach. In this paper we report spin-density functional theory (SDFT) calculations for a slab geometry (see Fig. 1). We use the generalized gradient approximation (GGA)⁸ for the exchange-correlation functional and the full-potential linearized augmented plane wave (FP-LAPW) method^{9,10} to solve the Kohn-Sham equations. The STM study was performed on a thin hematite film grown epitaxially onto a Pt (111) substrate.

The identification of thermal equilibrium structures of surfaces is a prerequisite for an understanding of the endurance, electronic, magnetic, and chemical properties of the material. For a two-component material, as Fe_2O_3 ,

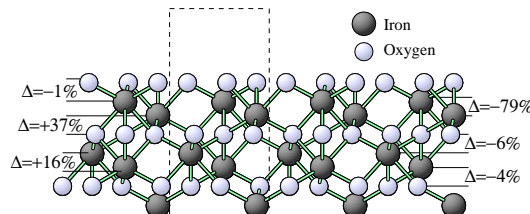


FIG. 1. Upper half of the slab for the unrelaxed O_3 -terminated surface. The cross section of the upper half of the supercell is noted by the dashed rectangle. The Δ indicate the calculated interlayer relaxations in % relative to an unrelaxed surface, i.e., a truncated bulk geometry.

under realistic conditions the surface will exchange atoms with chemical reservoirs. Therefore we will analyze the Gibbs free energy with its dependence on the chemical potentials of the two components. For metal oxides, it is obvious that the O_2 partial pressure is the practical handle on this dependence. Interestingly, neither experimental nor theoretical studies have identified the composition and structure of surfaces of Fe_2O_3 so far, and it is unknown how the surface structure depends on the oxygen chemical potential. In this paper we show that the surface properties change significantly with O_2 pressure and that under typical oxygen pressure conditions two chemically distinct domains are likely to exist.

The $\alpha\text{-Fe}_2\text{O}_3$ crystallizes in the hexagonal corundum structure, where the primitive bulk unit cell contains six formula units (30 atoms). Along the [0001] axis this structure can be viewed as a stack of Fe and O_3 layers: $\cdots\text{Fe-Fe-O}_3\text{-Fe-Fe-O}_3\cdots$. The (0001) surface is stable and often occurs on naturally grown crystals¹¹. It exhibits an unreconstructed (1×1) surface with a hexagonal unit cell^{12,13}. In the total-energy calculations we considered the following (likely) surface terminations with (1×1) periodicity: $\text{Fe-Fe-O}_3\cdots$, $\text{Fe-O}_3\text{-Fe}\cdots$, $\text{O}_3\text{-Fe-Fe}\cdots$, $\text{O}_2\text{-Fe-Fe}\cdots$, $\text{O}_1\text{-Fe-Fe}\cdots$, where the latter two surfaces correspond to an oxygen termination with oxygen vacancies. For the $\text{Fe-O}_3\text{-Fe}\cdots$ terminations we considered all four possible geometries of the surface Fe, and find that the energetically favorable surface is that with the top Fe site

occupied according to the bulk stacking sequence. Figure 1 shows as an example our slab for the O_3 -Fe-Fe-... surface study. We find that two of the five candidates considered have a particularly low energy and predict that both should be present under typical experimental conditions. These are the Fe-O₃-Fe-... and the O₃-Fe-Fe-... structures. The low energy of the Fe-O₃-Fe-... surface is consistent with recent findings for other corundum type materials (Al₂O₃¹⁴ and Cr₂O₃¹⁵), but for Fe₂O₃ it had not been identified so far. The other structure which we predict, *i.e.* the termination by O₃, is unexpected in general (also for other corundum type crystals) because this termination suggests a high surface dipole moment and thus an electrostatically unfavorable situation. In fact, our calculations reveal that this argument, which is based on the understanding of the bulk properties of Fe₂O₃, is too simple for describing the surface. Indeed, both low-energy surface structures are stabilized by a significant surface relaxation which implies that the surface should be viewed as a “new material”, not just a truncated bulk.

For the FP-LAPW calculations we use a kinetic-energy cutoff for the plane-wave basis of $E_{\text{max}}^{\text{wf}} = 18$ Ry. This is a rather high value and makes the calculations very involved. However, because of the huge surface relaxations found in the course of this study we had to use rather small muffin-tin spheres ($R_{\text{Fe}}^{\text{MT}} = 0.95$ Å, $R_{\text{O}}^{\text{MT}} = 0.74$ Å) and therefore a large value for $E_{\text{max}}^{\text{wf}}$ was mandatory to ensure good numerical accuracy. Details of the calculations are presented elsewhere. The bulk as well as the surface calculations were performed with a hexagonal unit cell and a uniform \mathbf{k} -point mesh with five points in the irreducible part of the Brillouin zone. All parameters defining the numerical accuracy of the calculations were carefully tested. For the bulk we obtain the following results (experimental values¹⁶ in parentheses): $a_0 = 5.025$ (5.035) Å, $c_0 = 13.671$ (13.747) Å, $z(\text{Fe}) = 0.357$ (0.355) Å, $x(\text{O}) = 0.308$ (0.306) Å. Our calculations give an antiferromagnetic ordering with a local moment of $M = 3.39\mu_B$ (considering the contribution from the muffin tin only). The spins are pointing parallel to [0001], and in the Fe-Fe double layers are aligned parallel. But between neighboring double layers (separated by an O₃ layer) the spins are antiparallel. Our result is similar to recent bulk calculations using the augmented spherical wave method¹⁷, but the magnetic moment are smaller than the experimental values $M = 4.6$ - $4.9\mu_B$ ^{18,19}. This difference was blamed on difficulties of the experimental analysis^{20,17}. The heat of formation per Fe₂O₃ unit is 8.024 (8.48)²¹ eV. The slabs consist of six O₃ layers and ten, twelve, or fourteen Fe layers, depending on the surface termination to be studied (see Fig. 1 as one example). All atoms of the slab are allowed to relax and no symmetry restrictions are applied. The antiferromagnetic ordering is found to remain up to the surface.

The Gibbs free energy Ω of the slab at temperature T and partial pressure p is given by

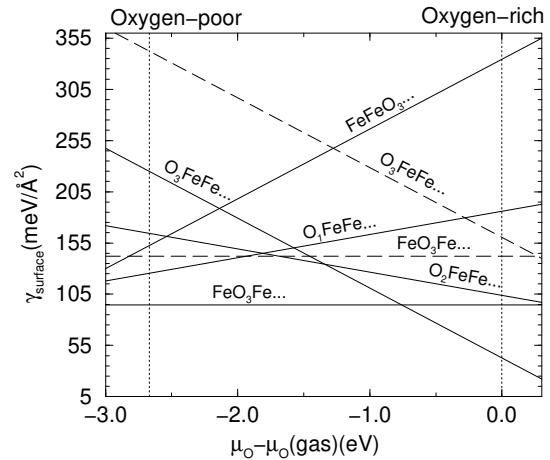


FIG. 2. Surface energies of different Fe₂O₃(0001) surface terminations. $\mu_{\text{O}}(\text{gas})$ is the chemical potential per oxygen atom of molecular O₂. The allowed range of $\mu_{\text{O}} - \mu_{\text{O}}(\text{gas})$ is indicated by the vertical dotted lines, where the left one corresponds to strongly Fe-rich (*i.e.*, oxygen-poor) conditions, and the right one corresponds to strongly oxygen-rich conditions (*i.e.*, high oxygen gas pressure). Full lines show results for relaxed geometries, and dashed lines give for comparison results for unrelaxed surfaces.

$$\Omega = E^{\text{total}} + pV - TS - \mu_{\text{Fe}}N_{\text{Fe}} - \mu_{\text{O}}N_{\text{O}} \quad , \quad (1)$$

where E^{total} is the total energy of the slab, μ_{Fe} the chemical potential of iron, and μ_{O} the chemical potential of oxygen. N_{Fe} and N_{O} are the number of iron and oxygen atoms of the supercell. For typical pressure and temperature, the pV and TS terms in Eq. 1 can be neglected. The Fe and O chemical potential are not independent, because they are related to each other by the existence of the Fe₂O₃ bulk phase. This gives

$$\Omega = E^{\text{total}} - \frac{1}{2}N_{\text{Fe}}\mu_{\text{Fe}_2\text{O}_3(\text{bulk})} + \left(\frac{3}{2}N_{\text{Fe}} - N_{\text{O}}\right)\mu_{\text{O}} \quad , \quad (2)$$

where $\mu_{\text{Fe}_2\text{O}_3(\text{bulk})}$ is the total energy per bulk Fe₂O₃ formula unit (with 2 Fe and 3 O atoms).

In Fig. 2 we show our results of Eq. 2 for various (1 × 1) geometries, where γ is the Gibbs free energy per surface area. The meaningful range of $\mu_{\text{O}} - \mu_{\text{O}}(\text{gas})$ is limited by the conditions that the chemical potential of Fe has to be smaller than that of an atom of bulk iron, and the chemical potential of oxygen has to be smaller than that of an oxygen atom of O₂. Otherwise an iron or oxygen condensate will form at the surface. The allowed range of the oxygen chemical potential, $\mu_{\text{O}} - \mu_{\text{O}}(\text{gas})$, is marked in Fig. 2 by the vertical dotted lines.

The results show that the Fe and the O₃ terminated surfaces are particularly stable. The relaxation energy is significant, in particular for the O₃ termination. In fact, from these results we predict that under typical experimental conditions the surface should consist of two domains, with these two structures. The O₃ termination has not been discussed before but for the Fe-O₃-Fe-... termination semi-empirical studies had been per-

TABLE I. Interlayer relaxations at the Fe-O₃-... and O₃-Fe-... surface relative to the corresponding bulk spacings.

interlayer	Fe-O ₃ -...			interlayer	O ₃ -Fe-... present
	present	Ref. 5	Ref. 6		
Fe-O ₃	1-2	-57%	+1%	-49%	
O ₃ -Fe	2-3	+7%	+5%	-3%	1-2
Fe-Fe	3-4	-33%	-47%	-41%	2-3
Fe-O ₃	4-5	+15%	+20%	+21%	3-4
O ₃ -Fe	5-6	+5%	+3%	-	4-5
Fe-Fe	6-7	-3%	+2%	-	5-6
Fe-O ₃	7-8	+1%	-	-	6-7
O ₃ -Fe	8-9	+4%	-	-	7-8

formed. Our surface energy for the relaxed geometry is $1.52 \text{ J/m}^2 = 94.58 \text{ meV/\AA}$ which is in close agreement with the semi-empirical studies of Mackrodt *et al.*⁵, who obtained 1.53 J/m^2 , and Wasserman *et al.*⁶, who obtained 1.65 J/m^2 . Also other corundum-type materials have a comparable surface energy for the (0001) surface: For α -Al₂O₃ Manassidis *et al.*²² obtained 1.76 J/m^2 , and Rohr *et al.*¹⁵ obtained for Cr₂O₃ a value of 1.60 J/m^2 .

Table I collects the calculated surface relaxations for the Fe-terminated surface. We obtain a relaxation pattern which alternates when going away from the surface. For the Fe terminated surface, the comparison with previous (semiempirical) studies reveals that a model using static ions⁵ is not appropriate, but when some polarization is allowed⁶, the system is apparently well described. In fact, our calculation shows that at the surface the covalent contribution to bonding is enhanced, which is mainly due to a hybridization of O *2p* and Fe *3d* orbitals. The workfunction of the Fe terminated surface is calculated as 4.3 eV (before relaxation it is only 3.1 eV). Recently, in a LEED analysis for Cr₂O₃ Rohr *et al.*¹⁵ determined a 60 % reduction for the first Cr-O₃ interlayer distance, which is in surprisingly close agreement with our result for Fe₂O₃ (we obtain 57 %). A detailed list with the geometry data which we obtained will be given elsewhere. Here we only note that the O₃ triangles of the first oxygen layer, *i.e.* the second layer from the surface, exhibit a clock-wise rotation by 2° without breaking the C₃ surface symmetry. No LEED analysis for the Fe-terminated (0001) surface of Fe₂O₃ exists so far.

The O₃ terminated surface (see Figs. 1 and 2) is indeed a very unexpected system and only stabilized by huge and unusual relaxations which are collected in Table I. The top layer O₃ triangles undergo a significant rotation (by 10°) without breaking the C₃ surface symmetry. The oxygen atoms remain nearly planar. Similarly to the Fe-terminated surface, a very notable feature is the contraction of the first subsurface Fe-Fe interlayer spacing, followed by an expansion of the next Fe-O₃ spacing. The huge interlayer relaxations and the O₃ rotational reconstruction provide the important contribution to the decrease of the surface energy and stabilize the O₃-terminated surface. As mentioned above, the stability of

this surface cannot be understood in terms of a simple ionic model, in which the surface oxygen atoms were negatively charged. Indeed, according to our calculations the ionic character of the O atoms is decreased at the O₃-terminated surface, and the covalent interaction between O *2p* and Fe *3d* states is enhanced significantly. This is also reflected in a noticeable *decrease* of the work function upon relaxation (from 8.3 eV to 7.6 eV).

The surface relaxations and change in the nature of bonding at the surface goes hand in hand with a dramatic change in the magnetic properties. Here, we discuss the integral over the magnetization density considering the contribution from inside the muffin-tin spheres. Therefore the direct values should not be taken too literally. But differences in moments between different layers and between the relaxed and unrelaxed situation are indeed meaningful. For the Fe-terminated surface we find that the magnetic moment of the topmost Fe layer is reduced against the bulk value by about 7 % (namely $\Delta M = -0.24\mu_B$).

The electronic and magnetic properties of the O₃-terminated surface are unprecedented. We find that the subsurface iron layers change their character significantly. The local magnetic moments of the first and second Fe layer are reduced to less than 50 % of the bulk values ($\Delta M = -1.79$ and $-1.75 \mu_B$ respectively), and again, a significant fraction of this reduction only occurs upon surface relaxation and reconstruction. Interestingly, also the top O₃ layer now attains a noticeable magnetic moment ($M=0.20 \mu_B$ per atom). In the bulk, the magnetic moment of oxygen atoms is zero. Our calculations show that the surface states for the O₃-terminated surface are of Fe *3d* character. They are partially occupied by the Fe *3d* electrons formerly with different spin, which results in the decrease of the local magnetic moments of the iron atoms. Our calculations also show that the surface state electrons of the iron atoms reaching through the topmost O layer may noticeably affect the surface reactivity.

The STM experiments were performed in an ultra-high vacuum system described in detail elsewhere²³. It is equipped with a sample transfer mechanism and a separate preparation chamber for performing high pressure oxidation treatments. Single crystalline α -Fe₂O₃(0001) films were grown onto a clean Pt(111) substrate surface. In a first step about 10 nm thick Fe₃O₄(111) magnetite films were prepared by repeated deposition of iron and subsequent oxidation for 2 min at temperatures around 950 K in 10⁻⁶ mbar oxygen partial pressure²⁴. Then a final oxidation at T=1100 K in 10⁻³ mbar oxygen partial pressure was performed for 10 min. The structure formed under these conditions was quenched by cooling down the sample to room temperature in the oxygen atmosphere. Then the oxygen was pumped off and the sample was transferred back into the analysis chamber and immediately studied by STM. These films exhibited no Auger contamination signals and sharp (1×1) LEED patterns¹². X-ray photoemission spectroscopy revealed only Fe³⁺ and no Fe²⁺ species, indicating the formation

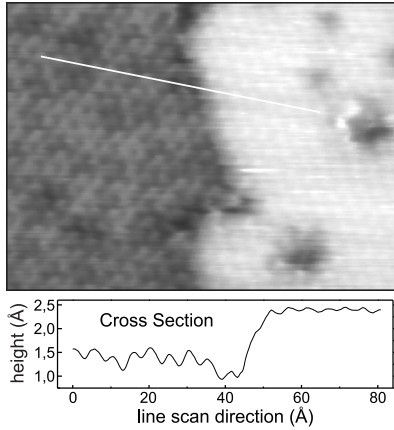


FIG. 3. Constant current image of an α - Fe_2O_3 (0001) surface prepared in 10^{-3} mbar oxygen partial pressure over an area of $100 \times 80 \text{ \AA}^2$ ($U = +1.3 \text{ V}$, $I = 1.3 \text{ nA}$). Below a cross section along the white line in the image is shown. Two different surface terminations can be seen.

of a single phase hematite film¹³.

Figure 3 shows an atomic resolution STM image of the α - Fe_2O_3 (0001) surface. A dark region and a bright region can be seen. They both exhibit hexagonal lattices formed by atomic protrusions with a periodicity of 5 \AA , which corresponds to the interatomic distance within the (0001) Fe-planes of the α - Fe_2O_3 structure. Below a cross section along the white line in the STM image is shown, which displays the 5 \AA periodicity and the two regions separated by a step about 1 \AA high. This step height considerably deviates from the distance between two equivalent (0001) surface terminations of α - Fe_2O_3 , which are separated by a monoatomic step with a height of 2.28 \AA . We always measure monoatomic steps or multiples of them between equivalent regions on the hematite surface. Therefore the two regions in Fig. 3 correspond to two different surface terminations that coexist on the α - Fe_2O_3 (0001) surface. This is further substantiated by their different corrugation amplitudes depicted in the cross section plot in Fig. 3, which are 0.1 and $0.2\text{-}0.3 \text{ \AA}$. Based on the apparent topographic height difference measured with the STM, we interpret the bright region as the Fe-terminated and the dark region as the O-terminated surface. About 20 % of the entire sample surface are covered by the bright termination as determined by numerous large-area scans. They form islands preferentially located near step edges on top of the dark termination, with sizes ranging between 20 and 200 \AA . We also confirmed that their formation depends on the oxygen partial pressure during the preparation (compare the discussion of Fig. 2 above). Measurements of STM spectroscopy, work function etc., and a detailed analysis of the dependence on oxygen pressure are in progress.

In summary, we have presented a detailed *ab initio* FP-LAPW study of the stoichiometry and structural relaxations of the α - Fe_2O_3 (hematite) (0001) surface. The

calculations predict two kinds of surfaces (thermal equilibrium with (1×1) symmetry), which depend on the growth conditions. We find a large inwards relaxation of the first layer for the Fe-terminated surface and a huge contraction of the interlayer spacing between the Fe subsurface layers for the O_3 -terminated surface. In addition to the relaxations along the [0001] direction, the O layers of both surfaces have a plane rotational reconstruction. To our knowledge, this is the first finding for such kind of special relaxations and plane reconstruction of oxygen layers at a metal-oxide surface. We also predict an unusual electronic structure of the O_3 -terminated surface with noticeable presence of states from the subsurface Fe layer. This also results in a magnetic polarization of the oxygen. With STM we confirm the existence of two different surface terminations coexisting on single crystalline hematite (0001) films, which have been prepared under a high oxygen pressure of 10^{-3} mbar.

-
- 1 T. Hirano, Appl. Catalysis **26**, 65 (1986).
 - 2 W. Weiss *et al.*, Catal. Lett. **52**, 215 (1998).
 - 3 L. L. Hu, T. Yoko, *et al.*, Thin Solid Films **219**, 18 (1992).
 - 4 T. Hashimoto, *et al.*, J. Ceram. Soc. Japan **101**, 64 (1993).
 - 5 W. C. Mackrodt, *et al.*, J. Cryst. Growth, **80**, 441 (1987).
 - 6 E. Wasserman, *et al.*, Surf. Sci. **385**, 217 (1997).
 - 7 L. Armelao, *et al.*, J. Phys.: Cond. Matt. **7**, L299 (1995).
 - 8 J. P. Perdew, *et al.*, Phys. Rev. B **46**, 6671 (1992).
 - 9 P. Blaha, *et al.*, Comput. Phys. Commun. **59**, 399 (1990).
 - 10 B. Kohler, *et al.*, Comput. Phys. Commun. **94**, 31 (1996).
 - 11 R. M. Cornell, *et al.*, (ed.), *The Iron Oxides*, VCH, Verlagsgesellschaft, (1996).
 - 12 W. Weiss, Surf. Sci. **377-379**, 943 (1997).
 - 13 Th. Schedel-Niedrig, *et al.*, Phys. Rev. B **52**, 17449 (1995).
 - 14 J. Guo, *et al.*, Phys. Rev. B **45**, 13647 (1992).
 - 15 F. Rohr, *et al.*, Surface Science **372**, L291 (1997).
 - 16 L. W. Finger, *et al.*, J. Appl. Phys. **51**, 5362 (1980).
 - 17 L. M. Sandratskii, *et al.*, J. Phys.: Condens. Matter **8**, 983 (1996).
 - 18 J.M.D. Coey *et al.*, J. Phys. C **4**, 2386 (1971).
 - 19 E. Kren, *et al.*, Phys. Lett. **19**, 103 (1965).
 - 20 D. D. Sarma *et al.*, Phys. Rev. Lett. **75**, 1126 (1995).
 - 21 CRC Handbook of Chemistry and Physics, edited by R. C. Weast, (CRC Press, Boca Raton, Florida, 1987), 67th ed.
 - 22 I. Manassidis, *et al.*, Surf. Sci. Lett. **285**, L517 (1993).
 - 23 W. Weiss, *et al.*, J. Vac. Sci. & Technol. A16(1), 21 (1998).
 - 24 W. Weiss, *et al.*, Phys. Rev. Lett. **71**, 1848 (1993).